http://dx.doi.org/10.5012/bkcs.2012.33.4.1269

Enhanced Visible Light Activity and Stability of TiO_2 Nanopowder by co-doped with Mo and N

Shaozheng Hu,* Fayun Li, and Zhiping Fan

Institute of Eco-environmental Sciences, Liaoning Shihua University, Fushun 113001, P. R. China
**E-mail: hushaozheng001@163.com*
Received December 15, 2011, Accepted January 16, 2012

A visible light responsive N, Mo co-doped TiO_2 were prepared by sol-gel method. X-ray diffraction, TEM, N_2 adsorption, UV-vis spectroscopy, photoluminescence, and X-ray photoelectron spectroscopy were used to characterize the prepared TiO_2 samples. Doping restrained the phase transformation from anatase to rutile and reduced the particle sizes. The band gap was much narrowed after N, Mo co-doping. The photocatalytic activities were tested in the degradation of an aqueous solution of a reactive dyestuff, methylene blue, under visible light. The photocatalytic activities of doped TiO_2 were much higher than that of neat TiO_2. The photocatalytic stability of N, Mo co-doped TiO_2 was much better than that of N doped TiO_2.

Key Words : co-doping, Molybdenum, TiO_2, Stability, Visible light

Introduction

Titanium dioxide has been a well-known photocatalytic material for the past few decades. TiO_2 with photocatalytic activity in the visible range is a great importance research topic in view of the applications in energy storage and environmental pollution control. However, because of the wide band gap of TiO_2 (*ca.* 3.2 eV for anatase), its practical application is inhibited for the low photon utilization efficiency and need of an UV excitation which accounts for only small fraction of the solar light (3-5%). Therefore, it is an important issue to develop new TiO_2 photocatalytic system with enhanced activities under visible light.

N doping into TiO_2 has been reported to be one of the most effective approaches to enhance the visible light activity. Asahi and coworkers claimed that the doped N atoms narrowed the band gap of TiO_2 by mixing N 2p and O 2p states, therefore demonstrating the activity for the decomposition of acetone and methylene blue.[1] Irie and coworkers systematically studied the relationship between the amount of doped-nitrogen and photocatalytic activity of N-doped TiO_2 for photooxidation of 2-propanol under visible light and ultraviolet irradiation.[2] They also suggested that the N 1s chemical state at 396 eV of N-doped TiO_2 is due to visible light response. However, Chen and Hu *et al.* reported that the photocatalytic activity of N doped TiO_2 was not stable.[3-6] The lattice-nitrogen was oxidated easily by photogenerated holes during the degradation reaction, leading to the decrease of activity.

It is reported that TiO_2 doped with transition metals could absorb visible light and exhibited high photocatalytic activity under visible light irradiation.[7] The result of Karakitsou and Verykios[8] showed that doping with cations with the valence higher than +4 can increase the photoactivity, whereas Mu *et al*.[9] reported that doping with trivalent or pentavalent metal ions was detrimental to the photoactivity even in the UV region. Furthermore, according to a systematic study on the photoactivity and transient absorption spectra of quantum-sized TiO_2 doped with 21 different metals the energy level and d-electron configuration of the dopants were found to govern the photoelectrochemical process in TiO_2.[10] Therefore, even though the effects of metal doping on the activity of TiO_2 have been a hot topic of investigation, it is still difficult to make unifiable conclusion on the effects of doping on photoactivities of TiO_2.

Recently, a lot of work have been reported on the metal and non-metal co-doped TiO_2.[11-13] Khana *et al*.[11] prepared B-Fe co-doped TiO_2. Huang e*t al*.[12] synthesized B-Ni co-doped TiO_2. Liu *et al*.[13] prepared Mo-N co-doped TiO_2. But the photocatalytic activity of the prepared catalyst was not investigated. In the present work, N, Mo co-doped TiO_2 was synthesized by the sol-gel method. The photocatalytic performance was evaluated in the degradation of methylene blue under visible light. The photocatalytic stability of prepared N, Mo co-doped TiO_2 was much better than the N doped TiO_2.

Experimental

Preparation and Characterization. In the experiment, all chemicals were analytical reagent grade. $(NH_4)_6Mo_7O_{24}\cdot 4H_2O$ was used as the precursor of N and Mo. 1 g Cetyl Trimethyl Ammonium Bromid (CTAB) was dissolved in a mixture of 10 mL Tetrabutyl Titanate (TTOB), 80 mL ethanol, and 6 mL nitric acid (70%) to make a homogeneous solution. Then 18 mL $(NH_4)_6Mo_7O_{24}\cdot 4H_2O$ solution (0.05 M) was added dropwise under strong stirring. The obtained sol was kept in oven at 50 °C for 48 h to get the gel. The obtained gel was calcined at 500 °C for 4 h to get the Mo, N co-doped TiO_2, which denoted as Mo-N-TiO_2. For comparison, neat TiO_2 was prepared by the same procedure described above but in the absence of $(NH_4)_6Mo_7O_{24}\cdot 4H_2O$. When $Na_2MoO_4\cdot 2H_2O$

or ammonia (with the same Mo/Ti and N/Ti ratio to $(NH_4)_6Mo_7O_{24}\cdot 4H_2O$) was used to replace $(NH_4)_6Mo_7O_{24}\cdot 4H_2O$ following the same procedure as in the synthesis of Mo-N-TiO_2, the product is denoted as Mo-TiO_2 and N-TiO_2, respectively. The mechanical mixing sample, MoO_3/TiO_2, was obtained by mixing the prepared neat TiO_2 and MoO_3 with the same Mo/Ti ratio to Mo-TiO_2.

XRD patterns of the prepared TiO_2 samples were recorded on a Rigaku D/max-2400 instrument using Cu-Kα radiation (λ = 1.54 Å). TEM images were measured using a Philips Tecnai G220 model microscope. UV-vis spectroscopy measurement was carried out on a Jasco V-550 spectrophotometer, using $BaSO_4$ as the reference sample. Nitrogen adsorption was measured at −196 °C on a Micromeritics 2010 analyzer. All the samples were degassed at 393 K before the measurement. BET Surface area (S_{BET}) was calculated according to the adsorption isotherm. Photoluminescence (PL) spectra were measured at room temperature with a fluorospectrophotometer (FP-6300) using an Xe lamp as excitation source. XPS measurements were conducted on a Thermo Escalab 250 XPS system with Al Kα radiation as the exciting source. The binding energies were calibrated by referencing the C 1s peak (284.6 eV) to reduce the sample charge effect.

Photocatalytic Reaction. Methylene blue (MB) was selected as model compound to evaluate the photocatalytic performance of the prepared TiO_2 particles in an aqueous solution under visible light irradiation. 0.1 g TiO_2 powders were dispersed in 100 mL aqueous solution of MB (50 ppm) in an ultrasound generator for 10 min. The suspension was transferred into a self-designed glass reactor, and stirred for 30 min in darkness to achieve the adsorption equilibrium. In the photoreaction under visible light irradiation, the suspension was exposed to a 110-W high-pressure sodium lamp with main emission in the range of 400-800 nm, and air was bubbled at 130 mL/min through the solution. The UV light portion of sodium lamp was filtered by 0.5 M $NaNO_2$ solution. All runs were conducted at ambient pressure and 30 °C. At given time intervals, 4 mL suspension was taken and immediately centrifuged to separate the liquid samples from the solid catalyst. The concentrations of MB before and after reaction were measured by means of a UV-vis spectrophotometer at a wavelength of 665 nm. The percentage of degradation D% was determined as follows:

$$D\% = \frac{A_0 - A}{A_0} \times 100\% \quad (1)$$

Where A_0 and A are the absorbances of the liquid sample before and after degradation, respectively.

Results and Discussion

The XRD patterns of neat TiO_2, N-TiO_2, Mo-TiO_2, and Mo-N-TiO_2 are shown in Figure 1. The phase contents and the particle sizes of the samples were calculated by their XRD patterns according to the method of Spurr[14] and Debye-Scherrer equation[15] respectively, and shown in Table 1. The neat TiO_2 was mixture of anatase and rutile phases. Whereas, after doping, the obtained samples were pure anatase phase. This indicated that doping restrained the phase transformation from anatase to rutile. The particle size of prepared TiO_2 sample was reduced appreciably after N doping, from 24 (TiO_2) to 21.5 nm (N-TiO_2). However, after Mo doping, the particle sizes of Mo-TiO_2 and Mo-N-TiO_2 are obviously decreased, from 24 to 15.6 and 13.3 nm. It is known that the ionic size of Mo^{6+} is almost equal to the Ti^{4+} ion, which can easily substitute Ti^{4+} in the TiO_2 lattice. Therefore, the decreased particle sizes of Mo-TiO_2 and Mo-N-TiO_2 could be probably due to the Mo doping which

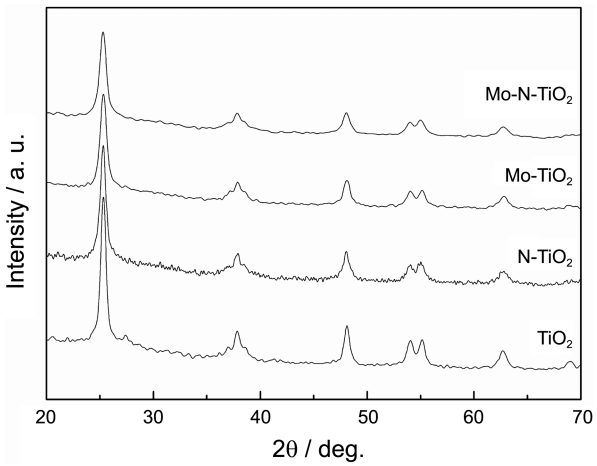

Figure 1. XRD patterns of neat and doped TiO_2 samples.

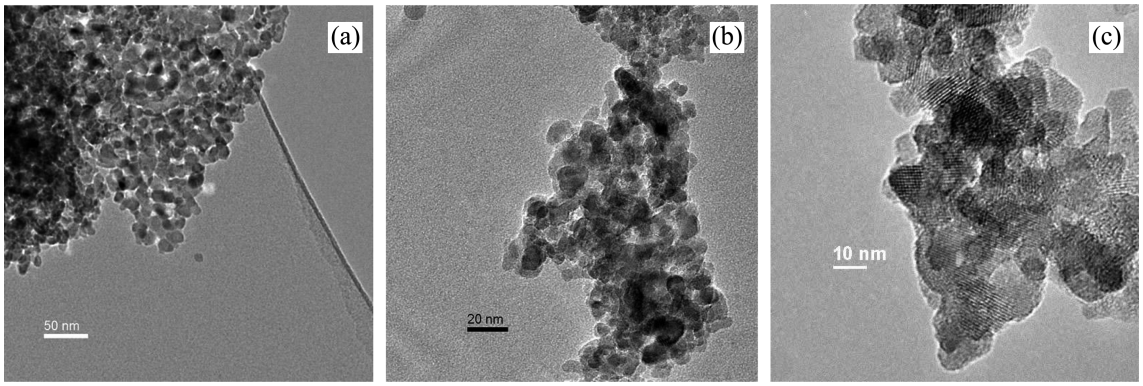

Figure 2. TEM images of neat TiO_2 (a), Mo-N-TiO_2 (b), and high magnification image of Mo-N-TiO_2 (c).

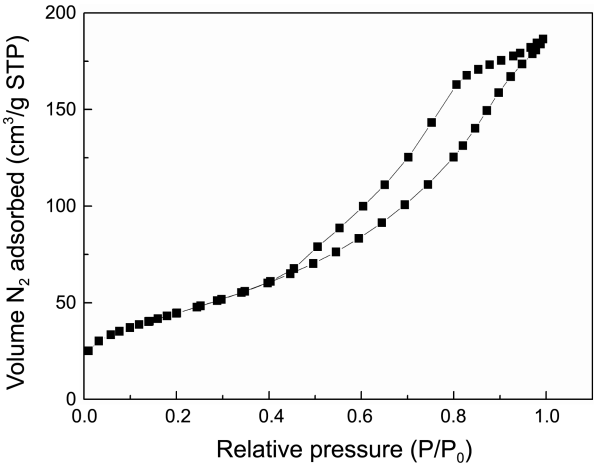

Figure 3. N_2 adsorption-desorption isotherm of Mo-N-TiO_2.

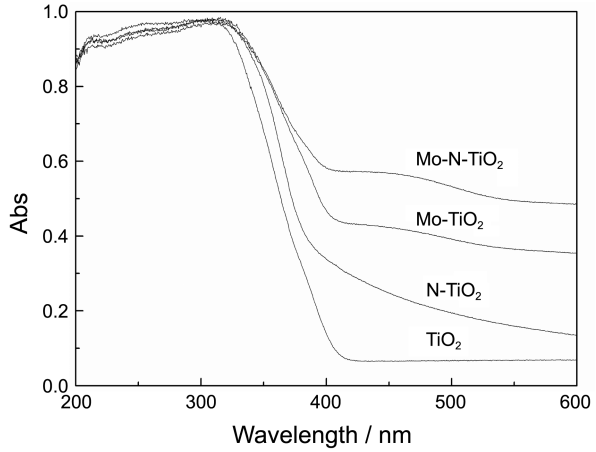

Figure 4. UV-vis diffuse reflectance spectra of neat and doped TiO_2 samples.

inhibits the growth of crystal grains.[16]

Figure 2 shows the representative TEM images of neat TiO_2 (a), Mo-N-TiO_2 (b), and high magnification image of Mo-N-TiO_2 (c). In Figure 2(a) and 2(b), the particle sizes of neat TiO_2 and Mo-N-TiO_2 were around 20-30 and 10-15 nm with the narrow particle size distribution. These are consistent with the XRD results. The high magnification image shows that Mo-N-TiO_2 was composed of highly ordered crystalline particles (Fig. 2(c)).

N_2 adsorption-desorption measurement indicates that mesoporous structure was present for all the TiO_2 samples. The N_2 adsorption-desorption isotherm of Mo-N-TiO_2, as a representative curve, is shown in Figure 3. The isotherm is of classical type IV, suggesting the presence of mesopores which formed by the addition of CTAB in the reaction solution.[17] The BET specific surface area (S_{BET}), pore volume, and central pore size are listed in Table 1. The S_{BET} and pore valume of Mo doped samples were much higher than that of others. Whereas, the opposite trend was observed for the central pore size (Table 1). These increased S_{BET} and pore volume might be attributed to the decreased particle sizes after Mo doping. The large S_{BET} and pore structure can promote adsorption, desorption, and diffusion of reactants and products, which is favorable to the photocatalytic performance.

Figure 4 shows the UV-vis spectra of neat and doped TiO_2 samples. Compared with the spectra of neat TiO_2 samples, obvious red-shifts of the absorption bands were observed for prepared doped TiO_2. The band-gap energies of TiO_2 samples which calculated according to the method of Oregan and Gratzel[18] (Table 1) indicate that the prepared doped TiO_2 samples exhibited much narrowed band-gap energies. According to the previous result,[1,16] this indicated that substitutional N and Mo atoms existed in the prepared doped TiO_2 samples. It is shown that Mo-N-TiO_2 exhibited the strongest visible light absorption. This strong absorption in the visible light region is of great importance for its practical application since it could be activated even by sunlight.

Table 1. Summary of physical properties of prepared TiO_2 samples

Sample	Size (nm)	X_A/X_R[a] (%)	S_{BET} (m^2g^{-1})	Pore volume (cm^3g^{-1})	Central Pore size (nm)	E_g (eV)
TiO_2	24	95 / 5	78	0.22	7.7	3.0
N-TiO_2	21.5	100 / 0	97	0.28	7.3	2.86
Mo-TiO_2	15.6	100 / 0	124	0.39	5.1	2.74
Mo-N-TiO_2	13.3	100 / 0	148	0.43	4.6	2.72

[a]X_A and X_R represent the phase composition of anatase and rutile, respectively.

XPS is an effective surface test technique for characterizing elemental composition and chemical states. The binding energy of the element is influenced by its electron density. A decrease in binding energy implies an increase of the electron density. Figure 5 shows the XP spectra of Mo-TiO_2 and Mo-N-TiO_2 in the region of Ti 2p (a), N 1s (b) and Mo 3d (c). In Figure 5(a), compared with Mo-TiO_2, slight shift to lower binding energy was observed for Mo-N-TiO_2. This is probably attributed to change of chemical environment after N doping.[19] The electrons of N atoms may be partially transferred from N to Ti, due to the higher electronegativity of oxygen, leading to increased electron density on Ti atoms. The presence of nitrogen species is evidenced by the N1s peak in the XPS spectrum of N-TiO_2 (Fig. 5(b)). Up to now, the assignment of the XPS peak of N1s is still under debate. Since the preparation methods and conditions considerably affect nitrogen XPS spectral features, the peak positions may be different from different literatures. In addition, the different nitrogen source may also influence the characteristics of the nitrogen state. Cong *et al.*[20] reported that the peak in the range of 397-401 eV was the N1s peak when using the wet chemical method. The N1s peaks of N-TiO_2 and Mo-N-TiO_2 are all around 399 eV, which are attributed to the N1s electron binding energy of the N atom in the environment of O-Ti-N.[21] These binding energies are higher than the typical binding energy of 396.9 eV in TiN. When nitrogen replaces the oxygen in the O-Ti-O structure, the electron density around N will be reduced. Thus, the N1s binding energy in an O-Ti-N environment is higher than that

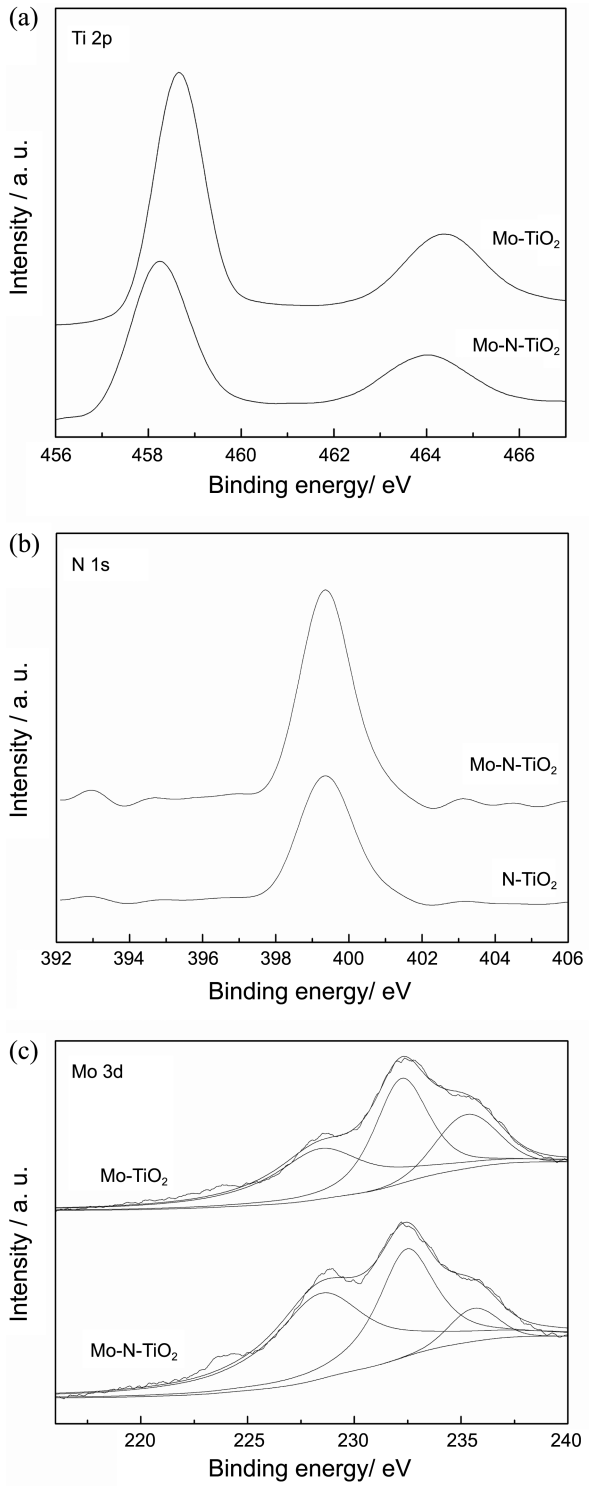

Figure 5. XP spectra of Mo-TiO_2 and Mo-N-TiO_2 in the region of Ti 2p (a), N 1s (b) and Mo 3d (c).

in an N-Ti-N environment. Besides, it is noted in Figure 5(b) that the peak intensity of Mo-N-TiO_2 is stronger than that of N-TiO_2, indicating more N atoms were doped in Mo-N-TiO_2 compared with N-TiO_2. This is probably due to that the doping of Mo atom cause the crystal lattice distortion, thus lead to the doping of N atom easier.

In Figure 5(c), the Mo 3d state can be fitted into three peaks, locating at 228.8, 232.6, and 236 eV, which can be further denoted to the oxidation states of Mo^{4+}, Mo^{5+}, and Mo^{6+}, respectively.[22] For MoO_3/TiO_2 sample (not shown here), only Mo^{6+} was observed. This indicated that not the mechanical mixing but the substitution of Mo atoms were occurred in Mo-TiO_2 and Mo-N-TiO_2. Besides, it is shown that more Mo^{4+} and less Mo^{6+} were formed in Mo-N-TiO_2 compared with Mo-TiO_2. This is probably attributed to that partial electrons of N atoms transferred from N to Mo, leading to more Mo^{4+} formed. It is reported that the oxidation-reduction potential of Mo^{6+}/Mo^{5+} is 0.4 eV and that of Ti^{4+}/Ti^{3+} is 0.1 eV,[23] so Mo^{6+} can capture photogenerated electrons more easily, thus can avail separate of carriers and enhance photocatalytic activity. The suitable amount dopants can capture photogenerated electrons and decrease the rate of recombination of electron-hole and accelerate photocatalytic reaction.

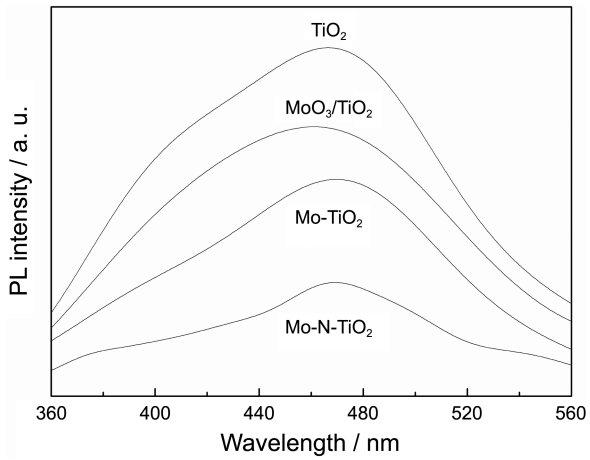

Figure 6. Photoluminescence emission spectra of neat TiO_2, Mo-TiO_2, MoO_3/TiO_2, and Mo-N-TiO_2.

PL emission spectrum, which is closely related to surface states and stoichiometric chemistry, is used to determine the efficiency of trapping, migration, and transfer of a charge carrier, and to understand the fate of electron-hole pairs in semiconductors. Figure 6 shows the PL spectra of neat TiO_2, Mo-TiO_2, MoO_3/TiO_2, and Mo-N-TiO_2. The PL intensity of prepared samples decreased in the order: TiO_2 > MoO_3/TiO_2 > Mo-TiO_2 > Mo-N-TiO_2. As the PL emission is the result of the recombination of excited electrons and holes, the lower PL intensity indicates the decrease in recombination rate, thus higher photocatalytic activity.[24] Most of the electrons and holes recombine within a few nanoseconds in the absence of scavengers. If scavengers (such as Mo^{6+}) are present to trap the electrons or holes, the electron-hole recombination can be suppressed, leading to a photoluminescence quenching.

Figure 7 shows the photocatalytic performances of neat and doped TiO_2 samples in the degradation MB under visible light irradiation. It is indicated that doped TiO_2 samples showed much higher photocatalytic activities than that of neat TiO_2. This must results from the doping of N and Mo atoms in TiO_2, which gave rise to the narrowed band gap and

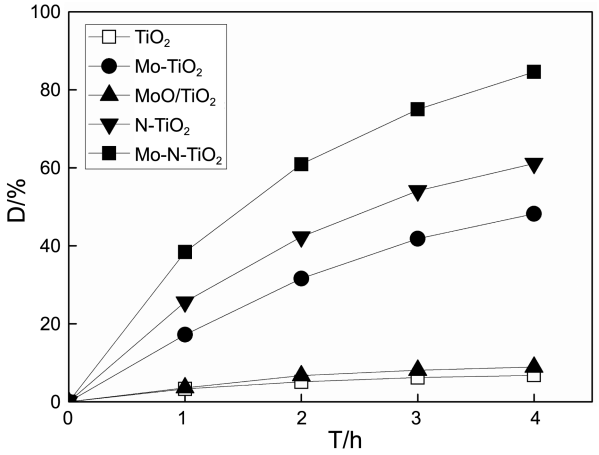

Figure 7. Photocatalytic performances of neat and doped TiO_2 samples in the degradation MB under visible light irradiation.

thus to the enhanced absorption in the visible region. The co-doped Mo-N-TiO_2 exhibited much higher photocatalytic activity than those doped with N or Mo alone. Besides, MoO_3/TiO_2 showed much lower activity than that of Mo-TiO_2 and Mo-N-TiO_2 indicating not the mechanical mixing but the substitution of Mo atoms were occurred in Mo-TiO_2 and Mo-N-TiO_2. This is consistent with XPS result.

Chen *et al*.[3] reported that the photocatalytic capability of N doped TiO_2 loses gradually due to the loss of doping N. The lattice-nitrogen was oxidated by photogenerated holes during the degradation reaction, leading to the photocatalytic instability. In this work, to check the photocatalytic stability, the photocatalytic performances of N-TiO_2 and Mo-N-TiO_2 under visible light were investigated in three cycles (Fig. 8). It is shown that Mo-N-TiO_2 exhibited no apparent decrease in photocatalytic activity after three cycles, which emphasizes the excellent photocatalytic stability. In contrast, the poor photocatalytic stability for N-TiO_2 is found, from 61% for fresh catalyst to 48% for 3rd reused catalyst. The doping N contents of N-TiO_2 and Mo-N-TiO_2 after three cycles were calculated according to the relevant XPS data (not shown here). The doping N content of N-TiO_2 decreased obviously

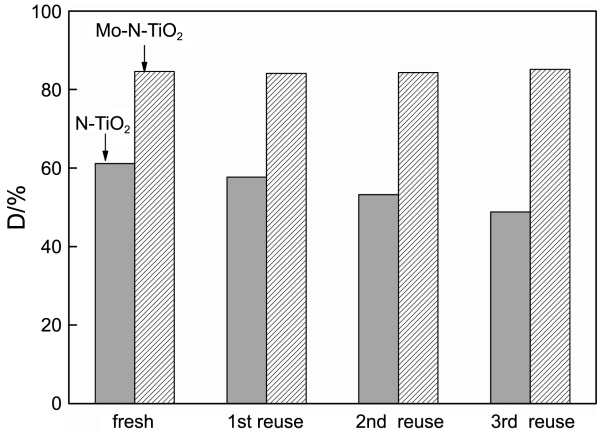

Figure 8. Photocatalytic stability of prepared N-TiO_2 and Mo-N-TiO_2 in the degradation of MB.

from 1.8 at.% to 1.2 at.% after three cycles. This confirmed the previous result that the doping N content significantly influenced the visible light activity.[25] However, no remarkable change was observed for Mo-N-TiO_2 in doping N content (2.0 and 1.88 at.% for fresh and 3rd reused catalyst), indicating that the lattice-nitrogen atoms in Mo-N-TiO_2 remained relatively stable. Devi *et al.* prepared Mo^{6+} doped TiO_2 and suggested that Mo^{6+} can react with h^+ to form Mo^{7+} which is highly unstable (Eq. 2).[16] The Mo^{7+} transfer the h^+ to the hydroxyl groups adsorbed on the catalyst surface at a faster rate and back to Mo^{6+} (Eq. 3). Therefore, it is deduced that the doping of Mo restrained the oxidation of lattice-nitrogen by the photogenerated h^+, thus increased the photocatalytic stability of Mo-N-TiO_2.

$$Mo^{+6} + h^+ \rightarrow Mo^{+7} \quad (2)$$

$$Mo^{+7} + OH^- \rightarrow Mo^{+6} + OH^{\bullet} \quad (3)$$

Conclusion

A visible light responsive N, Mo co-doped TiO_2 were prepared by sol-gel method. Doping restrained the phase transformation from anatase to rutile and reduced the particle sizes. The band gap was much narrowed after N, Mo co-doping. The photocatalytic activities of doped TiO_2 were much higher than that of neat TiO_2. Co-doped Mo-N-TiO_2 sample showed the highest activity. The photocatalytic stability of N, Mo co-doped TiO_2 was much better than that of N doped TiO_2. It is probably due to that the presence of Mo^{6+} restrained the oxidation of lattice-nitrogen by the photogenerated h^+, thus increased the photocatalytic stability of Mo-N-TiO_2.

Acknowledgments. This work was supported by National Natural Science Foundation of China (No. 41071317, 30972418), National Key Technology R & D Programme of China (No. 2007BAC16B07), the Natural Science Foundation of Liaoning Province (No. 20092080).

References

1. Asahi, R.; Morikawa, T.; Ohwaki, T.; Aoki, A.; Taga, Y. *Science* **2001**, *293*, 269.
2. Irie, H.; Watanaba, Y.; Hashimoto, K. *J. Phys. Chem. B* **2003**, *107*, 5483.
3. Chen, X. F.; Wang, X. C.; Hou, Y. D.; Huang, J. H.; Wu, L.; Fu, X. Z. *J. Catal*. **2008**, *255*, 59.
4. Hu, S. Z.; Li, F. Y.; Fan, Z. P. *Appl. Surf. Sci.* **2011**, *258*, 1249.
5. Hu, S. Z.; Li, F. Y.; Fan, Z. P. *Appl. Surf. Sci.* **2011**, *258*, 182.
6. Hu, S. Z.; Li, F. Y.; Fan, Z. P. *J. Hazard. Mater.* **2011**, *196*, 248.
7. Yamashita, H.; Harada, M.; Misaka, J.; Takeuchi, M.; Ikeue, K.; Anpo, M. *J. Photochem. Photobiol. A: Chem.* **2002**, *148*, 257.
8. Karakitsou, K. E.; Verykios, X. E. *J. Phys. Chem.* **1993**, *97*, 1184.
9. Mu, W.; Herrmann, J. M.; Pichat, P. *Catal. Lett.* **1989**, *3*, 73.
10. Choi, W.; Termin, A.; Hoffmann, M. R. *Phys. Chem.* **1994**, *98*, 13669.
11. Khana, R.; Kima, S. W.; Kim, T. J. *Mater. Chem. Phys.* **2008**, *112*, 167.
12. Huang, Y.; Ho, W. K.; Ai, Z. H. *Appl. Catal. B* **2009**, *89*, 398.
13. Liu, H. L.; Lu, Z. H.; Yue, L.; Liu, J.; Gan, Z. H.; Shu, C.; Zhang,

T.; Shi, J.; Xiong, R. *Appl. Surf. Sci.* **2011**, *257*, 9355.
14. Spurr, R. A.; Myers, H. *Anal. Chem.* **1957**, *29*, 760.
15. Lin, J.; Lin, Y.; Liu, P.; Meziani, M. J.; Allard, L. F.; Sun, Y. P. *J. Am. Chem. Soc.* **2002**, *124*, 11514.
16. Devi, L. G.; Kumar, S. G.; Murthy, B. N.; Kottam, N. *Catal. Commun.* **2009**, *10*, 794.
17. Sing, K. S. W.; Everett, D. H.; Haul, R. A. W.; Moscou, L.; Pierotti, R. A.; Rouquerol, J.; Siemieniewska, T. *Pure Appl. Chem.* **1985**, *57*, 603.
18. Oregan, B.; Gratzel, M. *Nature* **1991**, *353*, 737.
19. Li, H. X.; Li, J. X.; Huo, Y. N. *J. Phys. Chem. B* **2006**, *110*, 1559.
20. Cong, Y.; Zhang, J. L.; Chen, F.; Anpo, M.; He, D. N. *J. Phys. Chem. C* **2007**, *111*, 10618.
21. Hu, S. Z.; Wang, A. J.; Li, X.; Löwe, H. *J. Phys. Chem. Solids* **2010**, *71*, 156.
22. Khyzhun, O. Y. *J. Alloys Compounds* doi:10.1016/S0925-8388(03)00736-9.
23. Yang, Y.; Li, X. J.; Chen, J. T.; Wang, L. Y. *J. Photochem. Photobiol. A* **2004**, *163*, 517.
24. Hu, S. Z.; Wang, A. J.; Li, X.; Wang, Y.; Löwe, H. *Chem. Asian J.* **2010**, *5*, 1171.
25. Yamada, K.; Nakamura, H.; Matsushima, S.; Yamane, H.; Haishi, T.; Ohira, K.; Kumada, K. *C. R. Chimie* **2006**, *9*, 788.